Lipid A-modified *Escherichia coli* can produce porcine parvovirus virus-like particles with high immunogenicity and minimal endotoxin activity

Xuegang Shen[1†], Yong-Bo Yang[1,4†], Yanfei Gao[1†], Shujie Wang[1†], Haiwei Wang[1], Mingxia Sun[1], Fandan Meng[1], Yan-Dong Tang[1], Yabin Tu[1], Qingke Kong[2*], Tong-Qing An[1,3*] and Xue-Hui Cai[1,4*]

Abstract

Background A cost-effective *Escherichia coli* expression system has gained popularity for producing virus-like particle (VLP) vaccines. However, the challenge lies in balancing the endotoxin residue and removal costs, as residual endotoxins can cause inflammatory reactions in the body.

Results In this study, porcine parvovirus virus-like particles (PPV-VLPs) were successfully assembled from Decreased Endotoxic BL21 (BL21-DeE), and the effect of structural changes in the lipid A of BL21 on endotoxin activity, immunogenicity, and safety was investigated. The lipopolysaccharide purified from BL21-DeE produced lower IL-6 and TNF-α than that from wild-type BL21 (BL21-W) in both RAW264.7 cells and BALB/c mice. Additionally, mice immunized with PPV-VLP derived form BL21-DeE (BL21-DeE-VLP) showed significantly lower production of inflammatory factors and a smaller increase in body temperature within 3 h than those immunized with VLP from BL21-W (BL21-W-VLP) and endotoxin-removed VLP (ReE-VLP). Moreover, mice in the BL21-DeE-VLP immunized group had similar levels of serum antibodies as those in the BL21-W-VLP group but significantly higher levels than those in the ReE-VLP group. Furthermore, the liver, lungs, and kidneys showed no pathological damage compared with the BL21-W-VLP group.

Conclusion Overall, this study proposes a method for producing VLP with high immunogenicity and minimal endotoxin activity without chemical or physical endotoxin removal methods. This method could address the issue of endotoxin residues in the VLP and provide production benefits.

Keywords Porcine parvovirus, Virus-like particle, Minimal endotoxin activity, *Escherichia coli*, Lipid A

†Xuegang Shen, Yong-Bo Yang, Yanfei Gao and Shujie Wang are co-first authors and have contributed equally to this work.

*Correspondence:
Qingke Kong
kongqiki@163.com
Tong-Qing An
antongqing@caas.cn
Xue-Hui Cai
caixuehui@caas.cn

[1]State Key Laboratory for Animal Disease Control and Prevention, Harbin Veterinary Research Institute, Chinese Academy of Agricultural Sciences, No. 678 Haping Road, Xiangfang District, Harbin 150069, China
[2]College of Veterinary Medicine, Southwest University, No. 2 Tiansheng Road, Beibei District, Chongqing 400715, China
[3]Heilongjiang Provincial Key Laboratory of Veterinary Immunology, Harbin Veterinary Research Institute, Chinese Academy of Agricultural Sciences, Harbin 150069, China
[4]Heilongjiang Veterinary Biopharmaceutical Engineering Technology Research Center, Harbin Veterinary Research Institute, Chinese Academy of Agricultural Sciences, Harbin 150069, China

Introduction

Infectious diseases pose a substantial threat to public health, a concern highlighted by the recent COVID-19 outbreak [1]. Although conventional vaccines have been widely used for over a century, they are only available against a limited number of pathogens [2, 3]. Consequently, the emergence of new and variant pathogens has necessitated the development of vaccines to prevent and control the diseases caused by these pathogens. Subunit vaccines have gained prominence in recent years owing to their simple production methods, cost-effectiveness, and high level of safety [4]. The attribution of virus-like particle (VLP) vaccines as subunit vaccines has increased rapidly since their inception [5]. Currently, VLP vaccines play a crucial role in controlling and eliminating viral outbreaks in both humans and animals [6, 7]. VLPs consist solely of viral capsid protein and are devoid of genetic material. Their conformational epitopes, morphological structures, and antigenic epitopes are similar to those of natural virions, making them highly safe and immunogenic [8, 9]. Consequently, several VLP vaccines have been approved for veterinary or human use, many of which were produced using *Escherichia coli* (*E. coli*) expression systems. These include the bivalent human papillomavirus (HPV) VLP vaccine, hepatitis E virus (HEV) VLP vaccine, porcine foot-and-mouth disease type O vaccine, and bovine foot-and-mouth disease type O VLP vaccine [10–13]. Nanoscale VLPs have attracted considerable attention owing to their easy phagocytosis by antigen-presenting cells, which leads to increased immunogenicity.

A critical factor affecting the cost of vaccine development is the effectiveness of scaled-up production, which is influenced by the protein expression systems used [14]. Therefore, selecting an appropriate protein expression system is crucial for achieving optimal scale-up production. Prokaryotic expression systems such as *E. coli*, are commonly used for high-efficiency scaled-up production of recombinant proteins because of their low cost, high expression, and ease of separation from the purified product. Additionally, *E. coli* possesses a well-defined genetic background and is easily modified [15, 16]. It has also been successfully used in commercial subunit vaccines, such as the recombinant hepatitis E vaccine [17]. However, endotoxin residues are crucial factors that can substantially affect the safety of subunit vaccines [18].

Currently, endotoxins are removed through standard chemical and physical methods. However, these approaches are time-consuming, labor-intensive, and can cause considerable protein loss, and thus inefficient removal of endotoxins [19–21]. One potential solution to deal with endotoxin residues in subunit vaccines is the development of *E. coli* with low endotoxin activity [22, 23]. Endotoxins are released when bacteria lyse and die which can trigger fever in the body. They comprise three parts: a specific polysaccharide, a nonspecific core polysaccharide, and lipid A, and its endotoxin activity depends on lipid A [24–26]. Modifying the position or number of lipid acyl chains and removing phosphate groups can reduce endotoxin activity. However, these alterations may also impact bacterial growth and viability [27, 28]. Thus, it is crucial to balance the remodeling of the lipid A structure while maintaining the normal physiological state of the bacteria. Previous studies have attempted to reduce endotoxin activity by modifying the structure of *E. coli* lipid A [29, 30]. Liu et al. modified the lipid A structure by deleting *msbB28* and *pagP38* and inserting *pagL* and *lpxE* [31]. However, these studies did not simultaneously and systematically evaluate the endotoxin activity in vitro and in vivo [32].

Porcine parvovirus (PPV) infection, which often causes reproductive problems in pregnant sows, is common in pig farms worldwide. PPV vaccines can remarkably benefit modern intensive farms and improve their economic returns. Currently, available PPV vaccines are limited to traditional options, such as inactivated and attenuated vaccine [33, 34]. This highlights the necessity for a low-cost, safe, and effective VLP vaccine against PPV, which is currently being developed. Previous studies have successfully expressed the VP2 protein using *E. coli* BL21 and subsequently assembled PPV-VLP [35, 36]. Therefore, PPV-VLP was selected as the model VLP vaccine and will be used to assess the endotoxin activity and potential application of VLP purified from BL21 with structurally modified lipid A.

In this study, PPV-VLPs were expressed and purified in BL21 cells that have structurally modified lipid A. The endotoxin activities of lipopolysaccharide (LPS) and PPV-VLPs derived from Decreased Endotoxic BL21(BL21-DeE) and wild-type BL21 (BL21-W) cells were evaluated in vitro and in vivo. The immunogenicity and safety of PPV-VLPs purified from BL21-DeE cells were assessed in BALB/c mice. This study investigated whether BL21, with an altered lipid A structure, could be used as a potential production strain for subunit vaccines by effectively reducing endotoxin activity.

Materials and methods

Bacterial and culture conditions

The BL21-DeE, derived from the wild strain *E. coli* BL21(DE3), has its *msbB* and *pagP* genes knocked out. Additionally, *pagL* and *lpxE* genes were introduced to further modify LPS and produce monophosphorylated tetra-acylated lipid A [31]. The *msbB* gene encodes a ligase responsible for attaching a myristic acid moiety to lipid A, whereas the *pagP* gene encodes a ligase that catalyzes the addition of a palmitate chain to the hydroxyl group of the R-3'-hydroxymyristate chain at

the 2 position of lipid A [37–39]. Additionally, the *pagL* gene encodes an enzyme that hydrolyzes the ester bond at the lipid A position, thereby releasing the primary 3-hydroxymyristoyl moiety, and the *lpxE* gene encodes an inner membrane phosphatase that removes the 1'-phosphate group of lipid A in *E. coli* [40, 41]. This mutant strain was developed by Qingke Kong's research group and provided for this study. BL21(DE3) and DH5α strains were obtained from our laboratory collection (Table 1).

E. coli BL21 (DE3), BL21-DeE, and DH5α were cultured in lysogeny broth (LB) or LB agar at 37 °C. Kanamycin (Kan), chloramphenicol (Cm), and ampicillin (Amp) were added as necessary at 50, 25, and 100 μg/mL, respectively.

Purification of PPV-VLPs
PPV-VLPs were purified as previously described [35]. Briefly, the sonicated bacterial supernatant was precipitated with PEG 6000 and centrifuged at $12,000 \times g$ for 30 min. The resulting pellet was resuspended in 20 mM Tris-HCl (pH 8.0) and passed through a DEAE Bestrose Fast Flow column (Bestchrom, Zhejiang, China). The fractions of effluents containing VLPs were collected. To further separate the VLPs, a Sepharose 6FF 16/96 column (Bestchrom, Zhejiang, China) was used at a flow rate of 1.5 mL/min. Finally, the VLPs were passed through a heparin-agarose column (Bestchrom, Zhejiang, China) and eluted with a solution containing 500 mM NaCl and 20 mM Tris-HCl. Purified VLPs from BL21-W-VP2 and BL21-DeE-VP2 strains were named BL21-W-VLP and BL21-DeE-VLP, respectively. Subsequently, BL21-W-VLP was treated with Triton X-114 and named ReE-VLP. Protein eluates were analyzed by SDS-PAGE and western blot. For western blot, the membrane was transferred and blocked with 5% skim milk. Subsequently, the membrane was washed with PBST and incubated with PPV-positive serum (diluted at 1:5,000) for 2 h at 25 °C. After another round of PBST wash, the membrane was incubated with a fluorescently labeled pig secondary antibody (BD9448, Biotragon, Beijing, China; diluted at 1:10,000) for 1 h at 25 °C. Next, the membrane was subjected to another round of washing and then scanned and imaged using the Infrared Imaging System (Odyssey CLX, LI-COR, Nebraska, USA).

Morphological characterization of VLPs
Transmission electron microscopy (TEM) was performed to visualize the morphological characteristics of PPV-VLPs. The samples were adsorbed onto a copper grid and incubated at 25 °C for 10 min. Subsequently, 2.5% phosphotungstic acid solution was used to negatively stain the samples for 1 min. Any surplus stain was removed by blotting with filter paper, and the prepared samples were viewed under a transmission electron microscope (H-7650, Hitachi, Tokyo, Japan).

Hemagglutination assay of VLPs
Hemagglutination experiments were performed to compare the hemagglutination activities of BL21-W-VLP, BL21-DeE-VLP, and ReE-VLP. In this experiment, tenfold diluted VLPs of 12 serial gradients were added sequentially to a 96-well v-bottom plate containing 50 μL PBS in all wells. The mixture was then thoroughly mixed. Subsequently, 50 μL of 1% chicken red blood cell suspension was added to each well, and the mixture was thoroughly mixed. The plates were then incubated at 25 °C for 1 h. The highest dilution factor that exhibited complete agglutination was considered the hemocoagulation titer of PPV-VLPs.

Extraction and quantification of BL21-W and BL21-DeE LPS
The overnight cultures of BL21-W or BL21-DeE were transferred to 100 mL of LB medium containing the corresponding resistance at a ratio of 1:100, grown until OD_{600} reached approximately 0.9, and centrifuged for 10 min to collect the bacteria (4 °C, $10,956 \times g$). After washing the pellet twice with PBS, the bacteria were resuspended in 0.1 volume of PBS for ultrasonic disruption. Then, proteinase K (100 μg/mL) was added into the sonicated supernatant and incubated at 65 °C for 1 h. The mixture was added with 20% $MgSO_4$ (1 μL/mL), chloroform (4 μL/mL), 40 μg/mL RNase, and 20 μg/mL DNase for 37 °C overnight incubation. Next, an equal volume of preheated phenol was added to the solution, shocked for 30 min at 75 °C, incubated in an ice bath for 15 min, and centrifuged for 25 min ($9,000 \times g$). Then, the supernatant was collected, followed by adding ten volumes of absolute ethanol and incubating overnight at -20 °C to precipitate LPS. The cells were centrifuged for 15 min (3,000 ×

Table 1 Bacterial strains and plasmids used in the study

Strains or Plasmids	Information	Source
Strains		
E.coli BL21(DE3)	Protein expression	Laboratory collection
BL21-DeE	BL21(DE3)Δ*msbB28*Δ*pagP38* carrying pQK005, in which both *PagL* and *LpxE* were overexpressed under the lpp promoter in p15a plasmid backbone	Kong [31]
DH5α	Plasmid construction	Laboratory collection
Plasmids		
pET28a⁺-VP2	Protein expression	This study
pTf16-Amp	Expression of Trigger Factor to assist protein folding	This study
pTf16-Cm	Template for cloning the pTf16 backbone	Laboratory collection
pCold I	Template for cloning the *amp* gene	Laboratory collection

Shen *et al. Microbial Cell Factories*   (2024) 23:222

Page 4 of 13

g at 4 °C), and the precipitate was resuspended in ddH$_2$O. To obtain LPS, the resuspension was dialyzed overnight with two dialysate changes until the phenol in the aqueous phase was completely removed.

LPS quantification was optimized based on a published phenol sulfuric acid colorimetric method, whereby polysaccharides can be rapidly hydrolyzed to monosaccharides at the high temperature produced by the hydration of concentrated sulfuric acid to yield orange derivatives by reaction with phenol under strongly acidic conditions [42–45]. Briefly, 0.1 mg/mL glucose solution was diluted into 0, 20, 40, 60, 80, and 100 µg with ddH$_2$O. Then, 0.5 mL 5% phenol and 2.5 mL concentrated sulfuric acid were added. After incubation for 30 min, the absorbance of the dilutions was measured at 490 nm. The standard curve was plotted with glucose content as the abscissa and OD$_{490}$ values as the ordinate, and the average of three readings was calculated. The samples were analyzed using the same procedure, and the LPS concentration was calculated using the standard curve.

Endotoxin content detection

The endotoxin content of VLPs was detected using the Chromogenic LAL Endotoxin Assay Kit (C0276S, Beyotime, Beijing, China). Briefly, 10 µL sample in a microcentrifuge tube was added with 10 µL endotoxin detection reagent solution. The solution was then incubated in the dark at 37 °C for 9 min. Subsequently, 10 µL of chromogenic reagent solution was added, and the solution was incubated in the dark at 37 °C for 6 min. Next, 50 µL Buffer A, Buffer B, and Buffer C were sequentially added, allowing the solutions to stand for 5 min before measuring the absorbance at 545 nm using a microplate reader (Enspire, PerkinElmer, Connecticut, USA). Thorough mixing was done after adding each reagent.

Stimulatory effect of LPS on murine macrophage RAW264

The RAW264.7 cell line, derived from murine macrophages, was cultivated at 37 °C in an environment enriched with 5% CO$_2$. The growth medium consisted of dulbecco's modified eagle medium (DMEM) supplemented with 10% fetal bovine serum (FBS) and 100 µg/mL of gentamicin and penicillin. To maintain cell viability, the RAW264.7 cells were propagated to a concentration of 10^6/mL and subsequently seeded at 100 µL per well in 96-well plates. After incubating for 24 h, cells were stimulated with 3 and 6 µg of LPS, respectively. After another 24 h, the cells were centrifuged at 3,000 × g and 4 °C for 20 min to collect the supernatant. The corresponding Cytokine assay kit (MM-0132M1 and MM-0163M1, MEIMIAN, Jiangsu, China) was utilized to analyze the mouse TNF-α and IL-6 concentrations, following the manufacturer's instructions.

PPV-VLP vaccines preparation

To prepare the PPV-VLP vaccines, 100 µL of Montanide™ ISA 201 VG (SEPPIC) was added to 100 µL of purified PPV-VLP antigens at 25 °C following the manufacturer's instructions. This vaccine, consisting of 25 µg of VP2 antigen per 200 µL, was prepared under sterile conditions.

Animal experiments

All the animal experiments were conducted in accordance with the Guide for the Care and Use of Laboratory Animals of the Ministry of Science and Technology of the People's Republic of China, and the animal experiments (221205-02-GR) were performed under the supervision of the Committee on the Ethics of Animal Experiments of the Harbin Veterinary Research Institute (HVRI) of the Chinese Academy of Agricultural Sciences (CAAS).

To evaluate the immunogenicity of the PPV-VLP vaccines and the inflammatory response induced by LPS, 42 six-week-old female BALB/c mice were randomly allocated to six distinct groups. Mice in BL21-W-VLP, BL21-DeE-VLP, and ReE-VLP groups received 25 µg VLP vaccine via intramuscular injection in the leg, whereas one group was injected with PBS as a negative control. Protein concentrations were measured through BCA protein quantification. The remaining two groups were injected with LPS extracted from BL21-W or BL21-DeE cells. The injection volume for all groups was 200 µL. Booster immunization was administered on day 14 after the primary immunization. Blood samples were collected from the submandibular vein before and at specific intervals after the primary immunization (1 h, 3 h, 6 h, 12 h, day 35 and day 42). The body temperature of the vaccinated mice was measured 1, 3, and 6 h after the initial immunization.

Determination of antibody response and inflammatory cytokines

The specific IgG antibody against PPV-VP2 protein in the serum was determined through ELISA based on the VLP coatings developed in our laboratory [35]. This study used VLP as a coating agent (100 ng/well) in a 96-well ELISA. The microplates were incubated overnight at 4 °C, washed, and then blocked at 37 °C for 2 h. After washing, 100 µL serum sample (1:50 dilution) were added and incubated at 37 °C for 1 h. Subsequently, 100 µL HRP-SPA diluent (A0303, Beyotime, Beijing, China) was added at a ratio of 1:10,000 and incubated at 37 °C for another 1 h. Following another washing step, 100 µL tetramethylbenzidine (TMB, PR1200, Solarbio, Beijing, China) was added and incubated in a dark room at 37 °C for 15 min. All washing steps were performed thrice with PBST. Lastly, the reaction was terminated by adding 50 µL of stop solution (1 M HCl), and the absorbance was

measured at 450 nm. For IgG antibody titer test, collected sera were serially diluted and measured using ELISA method described above.

Serum neutralizing antibody titers were detected using live-virus assay method. Initially, the collected serum was inactivated at 56 °C for 1 h and diluted at various ratios (1:8, 1:16, 1:32, 1:64, 1:128, 1:256, 1:512, and 1:1024). Subsequently, 100 µL of the diluted serum was added to 96-well plate, along with 100 µL of a solution containing 200 TCID50 PPV. The plate was gently shaken and incubated at 37 °C for 1 h, and the mixture was then inoculated into a 96-well plate containing PK-15 cells. The cells were monitored daily over 5 days for cytopathic effect (CPE). The highest dilution of serum that prevented CPE was considered as serum neutralizing antibody titers to PPV.

The inflammatory cytokines (TNF-α and IL-6) in the serum of immunized mice (within 12 h after primary immunization) were detected using a Cytokine assay kit (MM-0132M1 and MM-0163M1, MEIMIAN, Jiangsu, China) according to the manufacturer's instructions.

Histopathological analysis of major organs from mice

Mice in the vaccine-immunized groups were euthanized 24 h after the initial immunization. Tissue samples (liver, lungs, kidneys, and intestines) were collected, preserved in 4% paraformaldehyde, and subjected to histopathological examination through H&E staining. This experiment was conducted by the Animal Disease Diagnostic Center (HVRI, CAAS, China) under appointment order no. BL 2022-0114bl.

Statistical analysis

GraphPad Prism version 9.5.1 (GraphPad Software, California, USA) was used to evaluate the significance of all values through one-way or two-way analysis of variance (ANOVA). The data were presented as the mean±SEM. A *p*-value greater than 0.05 indicated no significance (NS) among groups. To establish differences among experimental groups, the significance levels for statistical analyses were predetermined as $p < 0.05$ (*), $p < 0.01$ (**), $p < 0.001$ (***), and $p < 0.0001$ (****).

Results

Construction and expression of recombinant expression bacteria

Generally, chaperones facilitate protein folding and prevent protein aggregation and precipitation, increasing soluble protein expression in BL21 (DE3) cells. Previous studies have suggested that the pTf16-cm plasmid, which expresses chaperonin for chloramphenicol resistance, enhances the soluble expression of PPV-VP2 proteins and improves the efficiency of PPV-VLP assembly. To enable the expression of chloramphenicol-resistant

BL21-modified strains, the pTf16-cm plasmid was switched to ampicillin resistance and designated pTf16-Amp (Figure S1a). Agarose gel electrophoresis was performed to check pTf16-Amp expression. As shown in Figure S1b, the PCR-amplified bands of the two junctions of the pTf backbone and Amp fragment were detected using jian1-F1/jian1-R1 and JIAN2-F2/JIAN2-R2, respectively. To assess the growth of the engineered and wild-type strains expressing heterologous proteins, the growth curves of recombinant bacteria expressing PPV-VP2 proteins were determined. Figure 1a shows that BL21-DeE-VP2 and BL21-W-VP2 cells exhibited similar overall growth trends. However, at 10, 12, and 20 h into growth, the growth rate of BL21-DeE-VP2 was significantly lower compared to BL21-W-VP2 cells. Nevertheless, based on the comparable protein expression levels depicted in Fig. 1b, BL21-DeE-VP2 with low endotoxin levels remains suitable for applications involving PPV-VP2 expression. Additionally, the synthesis of the PPV-VP2 protein in the recombinant strains BL21-W-VP2 and BL21-DeE-VP2 was evaluated. SDS-PAGE analysis revealed bands of interest corresponding to the molecular weight of the VP2 protein (approximately 64 kDa) and pTf16 (approximately 56 kDa) in both strains (Fig. 1b). These results suggest that recombinant strains BL21-W-VP2 and BL21-DeE-VP2 effectively and consistently express PPV-VP2 protein with high stability and efficiency.

Purification and characterization of PPV-VLPs

To purify the PPV-VLPs, the sonicated bacterial supernatant of BL21-W-VP2 or BL21-DeE-VP2 strains was sequentially subjected to ion-exchange chromatography (IEC) and size-exclusion column chromatography (SEC). Furthermore, to evaluate the endotoxin-reducing effect of PPV-VLP from the BL21-DeE-VP2 strain on mice, endotoxin from the lysed BL21-W-VP2 supernatant was removed before purification using Triton X-114 was used as a control, and was denoted as ReE-VLP. As shown in Fig. 2a, the PPV-VLPs expressed in BL21-W-VP2 and BL21-DeE-VP2 strains exhibited high purity and yield after purification. SDS-PAGE results showed a single band corresponding to the expected molecular weight of VP2 (Fig. 2b). Western blot analysis confirmed the correctly folded PPV-VP2 proteins in BL21-W-VP2 and BL21-DeE-VP2 cells, and the structure was not altered after endotoxin removal using Triton X-114 (Fig. 2c). Uniformly intact particles approximately 25 nm in size were observed through TEM. Moreover, compared with BL21-W-VLP and BL21-DeE-VLP, Triton X-114-treated VLP displayed a lower quantity but higher purity, indicating that some VLPs were lost during endotoxin removal (Fig. 2d). The hemagglutination activity of BL21-W-VLP, BL21-DeE-VLP and ReE-VLP were 2^{10}(1:1024),
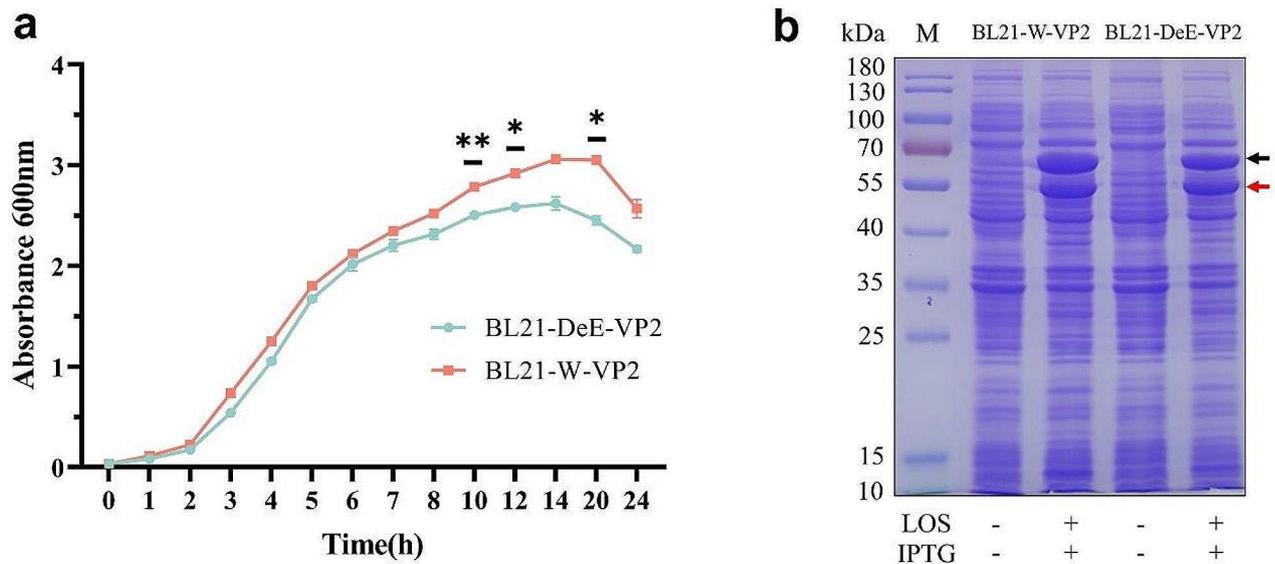
Fig. 1 Construction and expression of PPV-VP2 recombinant expression bacteria. **(a)** Growth comparison of BL21-DeE-VP2 and BL21-W-VP2 cells. The data are presented as mean ± standard deviation through two-way analysis of variance (ANOVA) using GraphPad Prism version 9.5.1; **(b)** PPV-VP2 expression in recombinant bacteria. Black and red arrows represent VP2 and pTf16 proteins, respectively, indicating that target bands are detected

2^9 (1:512), and 2^{11} (1:2048), respectively (Fig. 2e). These results suggest that all three VLPs share a similar structure with natural virions and correctly display the epitopes required for the hemagglutination activity of PPV.

BL21-DeE-LPS produces lower endotoxin toxicity in mice in vitro and in vivo

Lipid A is a major component of LPS and contributes to the secretion of proinflammatory cytokines. To explore the effect of varying the structure of lipid A on LPS content, the mass concentrations of purified LPS from BL21-W and BL21-DeE were determined through the phenol sulfuric acid method. The color depth of the aldol condensation reaction was positively correlated with mass concentration. LPS extracted from BL21-W and BL21-DeE was comparable in color depth to that after the phenol sulfuric acid reaction, and the statistical data showed no significant difference between them (BL21-W-LPS vs. BL21-DeE-LPS $p=0.9966$) (Fig. 3a). These results indicate that alterations in the lipid A structure have no significant effect on the LPS content of BL21, ruling out the interference of the LPS polysaccharide content of BL21-W and BL21-DeE on the inflammatory response in vitro and in vivo.

Additionally, inflammation is often accompanied by an increase in proinflammatory cytokines. LPS is a powerful inducer of inflammatory reactions in different mammalian cells, such as macrophages, monocytes, and endothelial cells. Previous studies have shown that LPS interacts with the CD14/TLR4/MD2 receptor complex, releasing the proinflammatory cytokines TNF-α

and IL-6 [46–48]. To further investigate the effect of LPS with structurally altered lipid A on the production of proinflammatory cytokines by mouse macrophages, RAW264.7 cells were stimulated with LPS derived from BL21-W and BL21-DeE, and the secretion of TNF-α and IL-6 in supernatants were evaluated by ELISA. As shown in Fig. 3b, the expression level of TNF-α in the BL21-W group was significantly higher than that in the BL21-DeE group at LPS doses of 3 and 6 μg. The differences were more pronounced with increasing stimulatory doses. Moreover, 3 μg LPS-stimulated cells resulted in no significant difference in the levels of IL-6 production between the BL21-W and BL21-DeE groups. However, a significant difference emerged when the dose increased to 6 μg (Fig. 3c). In addition, a 6 μg dose of LPS was used to evaluate proinflammatory cytokine production in BALB/c mice. As shown in Fig. 3d–e, the TNF-α and IL-6 produced by the BL21-W-LPS group were significantly higher than those in the BL21-DeE-LPS group within 3 h after LPS stimulation. In contrast, when LPS stimulation was extended to 6 h, the TNF-α exhibited no significant difference in the BL21-W-LPS and BL21-DeE-LPS groups, whereas IL-6 still showed a significant difference. These results showed that alteration of lipid A structure could decrease the production of TNF-α and IL-6 in LPS-stimulated cells in vitro and in vivo.

Antibody responses in BALB/c mice

To evaluate the immune responses to PPV-VLPs produced from BL21-W-VP2 and BL21-DeE-VP2 cells in vivo, mice were immunized with equal amounts of VLPs
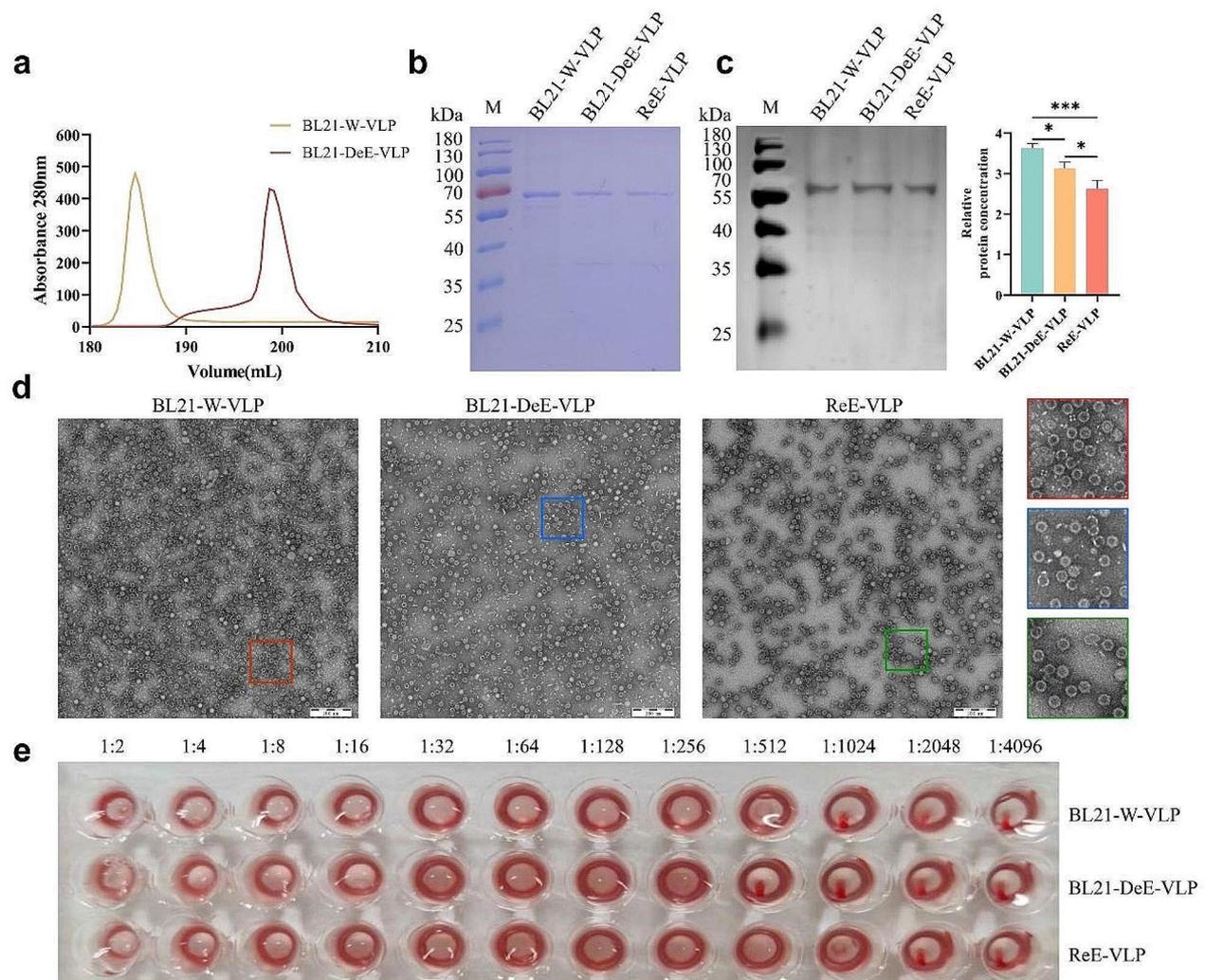
Fig. 2 Purification and characterization of PPV-VLPs. (**a**) Heparin-affinity profiles of PPV-VLPs purified from BL21-DeE-VP2 and BL21-W-VP2 with peaks representing correctly assembled VLPs. (**b**) PPV-VLPs purified from different strains were stained with Coomassie brilliant blue. ReE-VLP represents PPV-VLP treated with Triton X-114. (**c**) Western blot of PPV-VLPs purified from different strains. ReE-VLP represents PPV-VLP treated with Triton X-114. (**d**) The TEM images of PPV-VLPs purified from different strains, and the red, blue, and green boxes show the corresponding locally enlarged views. (**e**) Hemagglutination test of PPV-VLPs. Red agglutination is the hemagglutination titer of different PPV-VLPs

according to the immunization procedure (Fig. 4a). The endotoxin contents of BL21-W-VLP, BL21-DeE-VLP, and ReE-VLP were measured at 0.834 ± 0.002, 0.360 ± 0.001 and 0.460 ± 0.005 EU/mL, respectively (Fig. 4b-c). IgG antibodies, antibody titers, and neutralizing antibody titers in the sera of immunized mice were measured. IgG antibody detection revealed high levels of antibody production in the VLP groups compared with the PBS group on days 35 and 42 after primary immunization, and BL21-DeE-VLP and BL21-W-VLP antibody levels were significantly higher than those in the ReE-VLP group (Fig. 4d). To further confirm the antibody levels in the sera, IgG and neutralizing antibody titers were measured, which showed that although the antibody levels in the BL21-DeE-VLP and BL21-W-VLP groups were slightly higher than those in the ReE-VLP group, they were not

significantly different (Fig. 4e–f). These results indicate that PPV-VLP derived from the BL21-DeE strain was not significantly different from those derived from the wild-type strain in their ability to stimulate the organism to produce antibodies.

Mice immunized with the BL21-DeE-VLP vaccine produced lower TNF-α and IL-6 levels

To further compare the differences between VLPs purified from BL21-W and BL21-DeE in their ability to stimulate proinflammatory cytokine secretion, serum from mice at 1, 3, 6, and 12 h after primary immunization were collected to examine the levels of TNF-α and IL-6 (Fig. 5a). As shown in Fig. 5b, TNF-α produced by the BL21-DeE-VLP group were significantly lower than those in BL21-W-VLP and ReE-VLP groups within 12 h
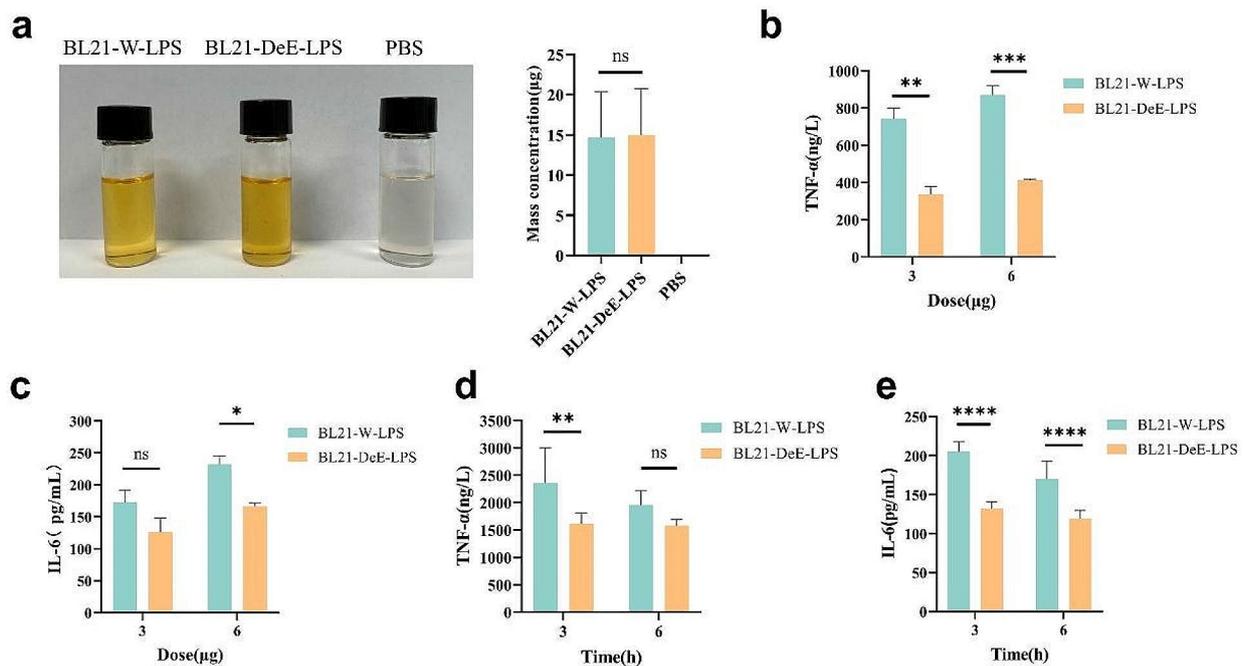
Fig. 3 Cytokine concentrations in RAW264.7 cells and mice blood after LPS stimulation. **(a)** Phenol sulfuric acid method was used to determine the mass concentration of purified LPS. The color depth represented the concentration, and OD490 showed no significant difference. **(b)** TNF-α levels in RAW264.7 cell supernatants were measured after 24 h of stimulation with varying concentrations of LPS; **(c)** IL-6 levels in RAW264.7 cell supernatants were measured after 24 h of stimulation with varying concentrations of LPS; **(d)** IL-6 concentration in blood of mice stimulated for 3 and 6 h with LPS; **(e)** TNF-α concentration in blood of mice stimulated for 3 and 6 h with LPS

post-immunization. In contrast, the production of IL-6 by the BL21-DeE-VLP group was significantly different from that of the BL21-W-VLP group within 6 h, whereas the difference from that of the ReE-VLP group was significant only at 3 h post-immunization (Fig. 5c). These results suggest that VLPs derived from the BL21-DeE strain stimulated the body to produce lower levels of pro-inflammatory cytokines than the wild-type strain.

Mice immunized with the BL21-DeE-VLP vaccine did not cause an increase in body temperature

The inflammatory response is often accompanied by an increase in body temperature. Previous studies have demonstrated that rats injected intraperitoneally with different types of *E. coli* LPS exhibit a significant rise in body temperature, peaking at approximately 6 h, compared with the negative control group [49]. To further probe the differences in body temperature induced by VLPs purified from lipid A-engineered BL21 and the wild strain, the body temperature of each immunized mouse was monitored at 1, 3, and 6 h post-immunization. Within 3 h, mice in the BL21-DeE-VLP group had notably lower body temperatures than those in the BL21-W-VLP and ReE-VLP groups (Fig. 6a). Within 6 h, except for the PBS group, whose body temperature did not change noticeable, all three groups tended to increase first and then

decrease, peaking at 3 h post-immunization (Fig. 6b). This result was consistent with previous findings [50], indicating that VLP derived from the BL21-DeE strain stimulated mice to produce lower body temperatures than the wild-type strain.

Mice immunized with the BL21-DeE-VLP vaccine did not cause obvious pathological organ damage

To further evaluate the pathological changes in mouse tissues in each group after immunization, the mice were euthanized 24 h after immunization, and the liver, lungs, intestines, and kidneys were harvested for pathological analysis. As shown in Fig. 7, no significant pathological lesions were observed in the liver, lungs, intestines, and kidneys of mice in the BL21-DeE-VLP and PBS groups. However, mice in the BL21-W-VLP group showed various degrees of pathological damage in all organs, except the intestine. The liver tissue showed extensive degeneration of hepatocytes with partial necrosis. The lung tissues exhibited extensive inflammatory cell infiltration, degeneration of bronchiolar epithelial cells, and edema of the vascular adventitia. The kidney tissue displayed tubular epithelial cell degeneration and pleomorphism. Furthermore, mice immunized with ReE-VLPs showed a few local inflammatory cell infiltrates in the lungs. However, other organs showed no obvious pathological damage.
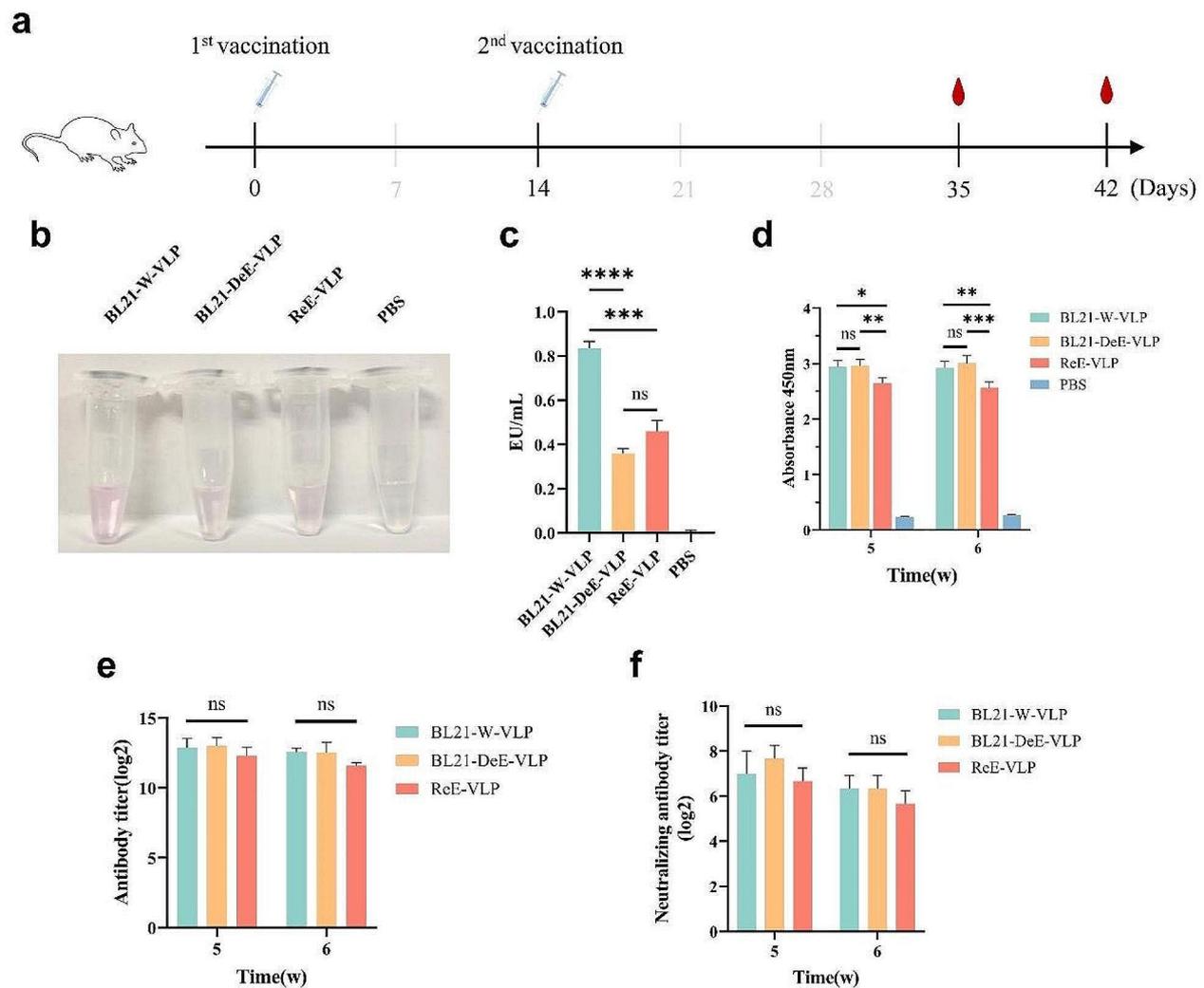
Fig. 4 Humoral immune response induced by PPV-VLPs in vivo. BALB/c mice (*n* = 7 per group) were immunized with different PPV-VLPs. Blood samples were collected to detect the production antibodies. Endotoxin content analysis of PPV-VLPs produced from BL21-W-VP2 and BL21-DeE-VP2 cells. **(a)** Schematic of mouse immune studies; **(b)** The image of PPV-VLPs after endotoxin content detection; **(c)** Quantitative analysis of endotoxin content of PPV-VLPs. **(d)** Serum concentrations of VP2-specific IgG was measured following two rounds of immunization with BL21-DeE-VLP, BL21-W-VLP, ReE-VLP, and PBS; **(e)** IgG antibody titers to VP2 in the sera of immunized mice was tested by ELISA; **(f)** Neutralizing antibody titers to PPV in the sera of immunized mice was measured by live-virus assay. Data are presented as mean ± SEM (*n* = 7)

These data demonstrated that VLP derived from the BL21-DeE strain significantly reduced pathological damage to murine tissues.

Discussion

Subunit vaccines derived from prokaryotic expression systems have economic advantages and play a crucial role in preventing and controlling porcine disease [51]. VLP vaccines that closely resemble the surface structures of natural viruses have been rapidly developed [5, 6, 52]. However, endotoxin residues cause inflammatory reactions, and complex and inefficient removal processes limit the development and application of such vaccines. Previous research has demonstrated that LPS with an altered lipid A structure can reduce endotoxin content and stimulate cells to produce low proinflammatory cytokine levels to maintain their adjuvanticity and immunological activity [53]. However, there has yet to be a systematic evaluation of the ability of lipid A-modified bacteria-derived subunit vaccines, such as VLP, to reduce the inflammatory response [32]. This study used BL21-DeE-LPS and BL21-DeE-VLP to assess inflammatory responses in vitro and in vivo. The findings indicated that BL21-DeE-LPS elicited lower levels of inflammatory factors in vitro and in vivo. More importantly, BL21-DeE-VLP demonstrated a significant reduction in the inflammatory response in mice compared with BL21-W-VLP, suggesting a promising avenue for clinical application.
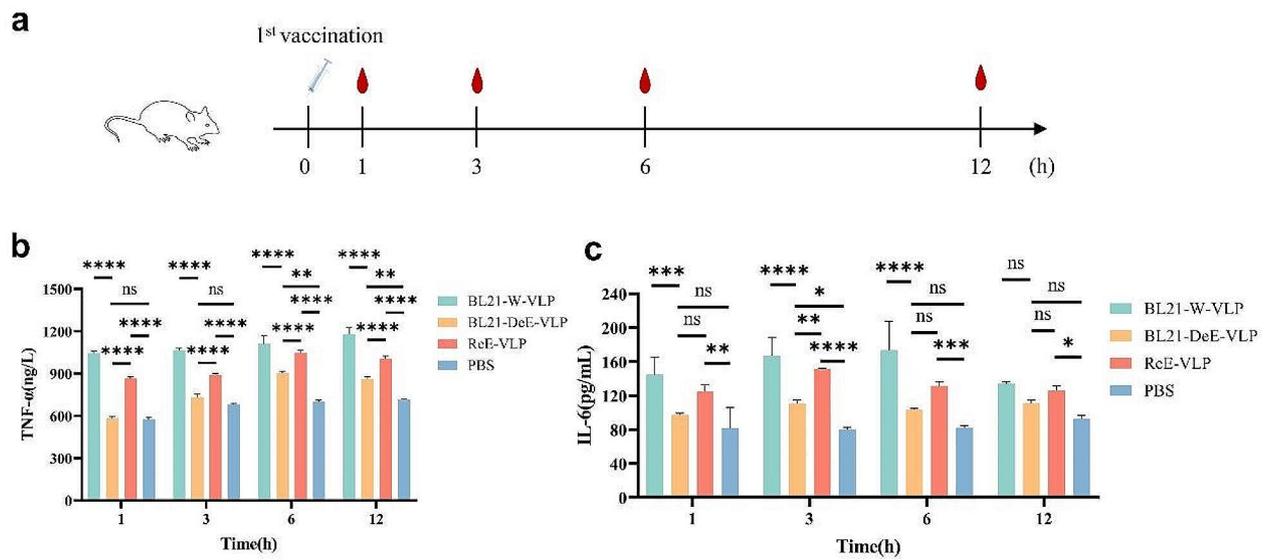
Fig. 5 Cytokine production induced by PPV-VLPs in vivo. BALB/c mice ($n=7$ per group) were immunized with different PPV-VLPs. Blood samples were collected to detect the production of cytokines. **(a)** Schematic of the sample collection procedure; **(b)** After one immunization with different PPV-VLPs, TNF-α concentration was detected by ELISA at 1, 3, 6, and 12 h, respectively; **(c)** After one immunization with different PPV-VLPs, IL-6 concentration was detected by ELISA at 1, 3, 6, and 12 h. Data are presented as mean ± SEM ($n=7$)
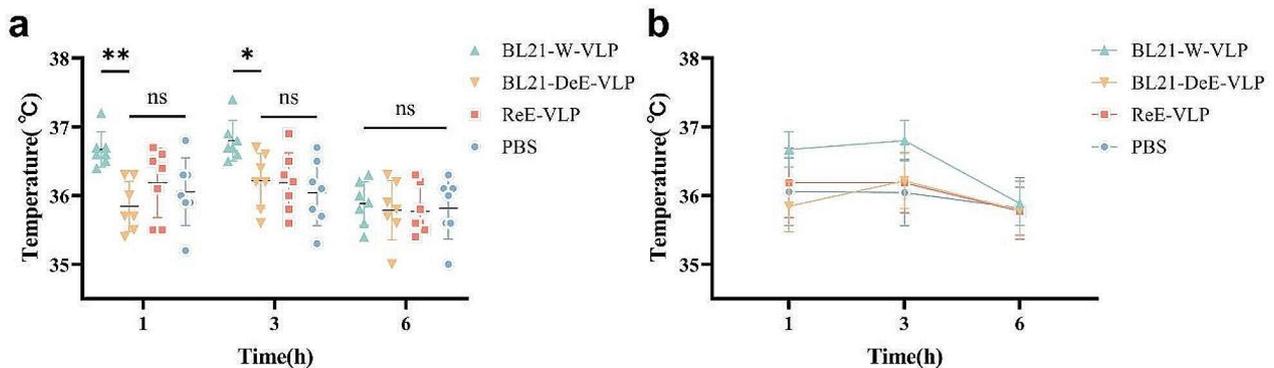
Fig. 6 Body temperature changes in PPV-VLP-immunized mice. **(a)** After immunization once with BL21-DeE-VLP, BL21-W-VLP, ReE-VLP, or PBS, the body temperature of each mouse was detected at 1, 3, and 6 h; **(b)** Statistics of temperature change trend in each group after immunization. Data are presented as mean ± SEM ($n=7$)

This study presented a direct method for purifying PPV-VLPs without additional endotoxin removal, which is advantageous for production. The uniform size and morphology of the BL21-DeE-VLP and BL21-W-VLP were confirmed by TEM (Fig. 2d). Interestingly, the number of ReE-VLPs treated with Triton X-114 and the column was significantly reduced compared with BL21-W-VLP (Fig. 2d), indicating that endotoxin removal treatment may cause sample loss. Moreover, the purified VLPs agglutinated with erythrocytes (Fig. 2e), indicating that BL21-DeE-VLP and BL21-W-VLP have similar surface antigen conformations.

The inflammatory response induced by endotoxins was evaluated using bacterial LPS and purified VLP.

The results showed that purified BL21-DeE-LPS stimulated RAW264.7 cells to produce significantly lower levels of IL-6 and TNF-α compared with BL21-W-LPS (Fig. 3b–c), which was consistent with previous studies [31]. This finding was further supported by an in vivo experiment in mice (Fig. 3d–e), which was important for evaluating the subsequent in vivo inflammatory response induced by BL21-DeE-VLP. We also evaluated the production of inflammatory factors, changes in body temperature, and the histopathology of BL21-DeE-VLP-immunized mice. The production of inflammatory factors in BL21-DeE-VLP-immunized mice was lower than that in mice immunized with BL21-W-VLP and ReE-VLP (Fig. 5b-c), indicating that LPS with an altered lipid
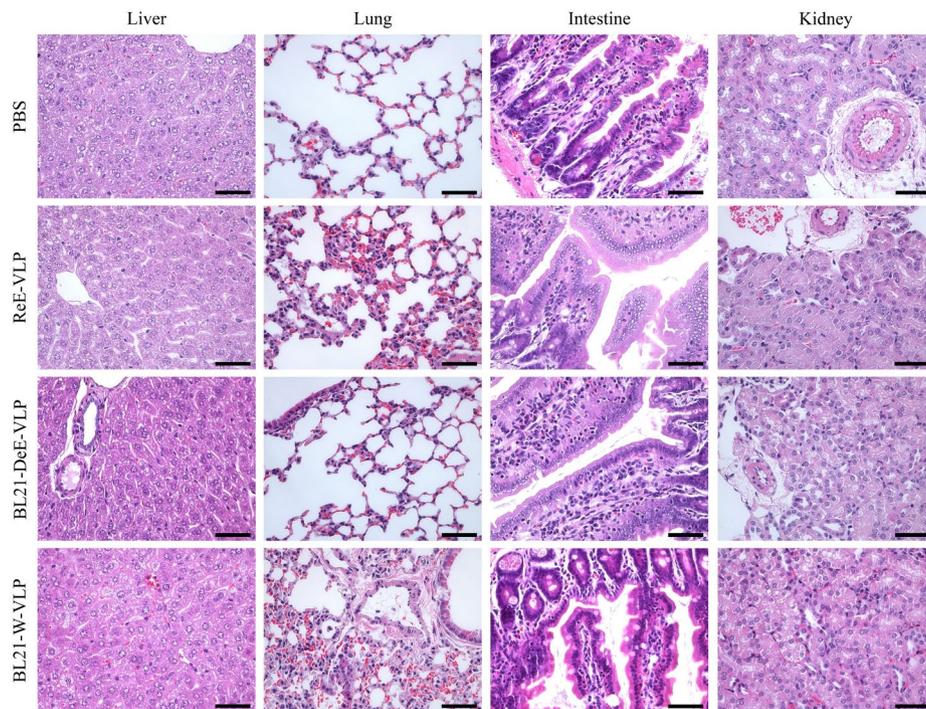
Fig. 7 Histopathological observation of PPV-VLP-immunized mice. The livers, lungs, intestines, and kidneys of mice in each group were collected 24 h after BL21-DeE-VLP, BL21-W-VLP, ReE-VLP, and PBS immunization

A structure had a better effect than chemical or physical methods in removing residual endotoxins from VLP. Within 3 h of immunization, the body temperature of BL21-DeE-VLP-immunized mice was significantly lower than that of BL21-W-VLP (Fig. 6a). Although there was no significant difference between the BL21-DeE-VLP and ReE-VLP groups, a decreasing trend was observed, which was consistent with the results of inflammatory factor production. In addition, the body temperature of immunized mice in the PBS group did not increase, whereas in the other three groups, the body temperature first increased and then returned to normal within 6 h (Fig. 6b). This result agrees with previous studies using LPS-induced inflammation models [50, 54]. However, compared with the BL21-DeE-VLP group, the BL21-W-VLP group showed varying degrees of pathological damage to the liver, lungs, and kidneys (Fig. 7). Additionally, a small amount of local inflammatory cell infiltration was observed in the lungs of ReE-VLP-immunized mice, suggesting that chemical or physical methods for removing residual endotoxins are unsatisfactory. These data indicate that VLP containing residual endotoxins can elicit an inflammatory response to a certain extent, and VLP purified from lipid A-modified bacteria is more effective in reducing the inflammatory response than endotoxin removal after purification.

Immunogenicity is a key indicator of VLP vaccine quality. The serum antibody detection results showed that the BL21-DeE-VLP immunized group was equivalent to the BL21-W-VLP group and significantly higher than the ReE-VLP group (Fig. 4d). This may be attributed to the presence of modified lipid A structure in the BL21-DeE-VLP immune group. Previous studies demonstrated that LPS is an effective immune adjuvant [55, 56]. In addition, some researchers have combined lipid A with antigens to enhance immunity [57, 58]. Notably, mice immunized with BL21-DeE-VLP exhibited a slight advantage in neutralizing antibody production compared with those immunized with ReE-VLPs (Fig. 4f), which may be attributed to the involvement of LPS.

The above results show that BL21, with a change in lipid A structure, can produce PPV-VLPs with low endotoxin activity. This finding can help address the challenge of removing endotoxin residues from VLP vaccines, which is currently complex and inefficient. However, the effectiveness of this approach should be tested using other subunit vaccines. Additionally, fermenting recombinant bacteria can provide insight into their production capacity at the fermentation level, which can serve as a basis for large-scale vaccine production.

Conclusions
In this study, we successfully purified PPV-VLPs from endotoxin-reduced BL21 cells and demonstrated a significant reduction in their ability to induce inflammatory responses in vitro and in vivo. This mutant strain can be

utilized to express VLP without eliminating LPS, offering a potential solution for addressing the issue of endotoxin residues in subunit vaccines, such as VLP.

Supplementary Information

Supplementary Material 1

Acknowledgements
Not applicable.

Author contributions
X.S. performed experiments, analyzed data, and wrote the manuscript. Y.Y. supervised experiments, interpreted data, conceptualized the study, and edited the manuscript. Y.G. performed experiments. S.W. led the immunogenicity experiments and interpreted data. H.W., M.S, and F.M. reviewed data and provided editorial comments on the manuscript. Y.T. provided the expression plasmid pET28a⁺-VP2. Q.K. provided the BL21-DeE strain and edited the manuscript. T.A., and X.C. designed, supervised experiments. All authors read and approved the final manuscript. X.S., Y.Y., Y.G. and S.W. contributed equally to this work.

Data availability
No datasets were generated or analysed during the current study.

Declarations

Ethics approval and consent to participate
This study was approved by the Committee on the Ethics of Animal Experiments of Harbin Veterinary Research Institute (HVRI) of the Chinese Academy of Agricultural Sciences (CAAS).

Consent for publication
All authors approve for publication.

Competing interests
The authors declare no competing interests.

References
1. Kola L, Kumar M, Kohrt BA, Fatodu T, Olayemi BA, Adefolarin AO. Strengthening public mental health during and after the acute phase of the COVID-19 pandemic. Lancet. 2022;399:1851–2.
2. Matić Z, Šantak M. Current view on novel vaccine technologies to combat human infectious diseases. Appl Microbiol Biotechnol. 2022;106:25–56.
3. Rappuoli R, Mandl CW, Black S, De Gregorio E. Vaccines for the twenty-first century society. Nat Rev Immunol. 2011;11:865–72.
4. Young A, Isaacs A, Scott CAP, Modhiran N, McMillan CLD, Cheung STM, Barr J, Marsh G, Thakur N, Bailey D, et al. A platform technology for generating subunit vaccines against diverse viral pathogens. Front Immunol. 2022;13:963023.
5. Mohsen MO, Zha L, Cabral-Miranda G, Bachmann MF. Major findings and recent advances in virus-like particle (VLP)-based vaccines. Semin Immunol. 2017;34:123–32.
6. Nooraei S, Bahrululolom H, Hoseini ZS, Katalani C, Hajizade A, Easton AJ, Ahmadian G. Virus-like particles: preparation, immunogenicity and their roles as nanovaccines and drug nanocarriers. J Nanobiotechnol. 2021;19:59.
7. Kheirvari M, Liu H, Tumban E. Virus-like particle vaccines and platforms for Vaccine Development. Viruses 2023, 15.
8. Yan D, Wei YQ, Guo HC, Sun SQ. The application of virus-like particles as vaccines and biological vehicles. Appl Microbiol Biotechnol. 2015;99:10415–32.
9. Mohsen MO, Bachmann MF. Virus-like particle vaccinology, from bench to bedside. Cell Mol Immunol. 2022;19:993–1011.
10. Chu K, Bi ZF, Huang WJ, Li YF, Zhang L, Yang CL, Jiang HM, Zang X, Chen Q, Liu DL et al. Safety and immunogenicity of an Escherichia coli-produced 9-valent human papillomavirus L1 virus-like particle vaccine (types 6/11/16/18/31/33/45/52/58) in healthy adults: an open-label, dose-escalation phase 1 clinical trial. *Lancet Reg Health West Pac* 2023, 34:100731.
11. Gupta J, Kumar A, Surjit M. Production of a Hepatitis E vaccine candidate using the Pichia pastoris expression system. Methods Mol Biol. 2022;2412:117–41.
12. Lee HW, Deng MC, Pan CH, Chang HW, Cheng IC. Neutralizing monoclonal antibodies against porcinophilic foot-and-mouth disease virus mapped to antigenic site 2 by utilizing novel mutagenic virus-like particles to detect the antigenic change. Vet Microbiol. 2018;222:124–31.
13. Chang J, Zhang Y, Yang D, Jiang Z, Wang F, Yu L. Potent neutralization activity against type O foot-and-mouth disease virus elicited by a conserved type O neutralizing epitope displayed on bovine parvovirus virus-like particles. J Gen Virol. 2019;100:187–98.
14. Pirkalkhoran S, Grabowska WR, Kashkoli HH, Mirhassani R, Guiliano D, Dolphin C, Khalili H. Bioengineering of antibody fragments: challenges and opportunities. Bioeng (Basel) 2023, 10.
15. Tungekar AA, Castillo-Corujo A, Ruddock LW. So you want to express your protein in Escherichia coli? Essays Biochem. 2021;65:247–60.
16. Du F, Liu YQ, Xu YS, Li ZJ, Wang YZ, Zhang ZX, Sun XM. Regulating the T7 RNA polymerase expression in E. Coli BL21 (DE3) to provide more host options for recombinant protein production. Microb Cell Fact. 2021;20:189.
17. Wen GP, He L, Tang ZM, Wang SL, Zhang X, Chen YZ, Lin X, Liu C, Chen JX, Ying D, et al. Quantitative evaluation of protective antibody response induced by hepatitis E vaccine in humans. Nat Commun. 2020;11:3971.
18. Singpant P, Tubsuwan A, Sakdee S, Ketterman AJ, Jearawiriyapaisarn N, Kurita R, Nakamura Y, Songdej D, Tangprasittipap A, Bhukhai K, et al. Recombinant Cas9 protein production in an endotoxin-free system and evaluation with editing the BCL11A gene in human cells. Protein Expr Purif. 2023;210:106313.
19. Wilding KM, Hunt JP, Wilkerson JW, Funk PJ, Swensen RL, Carver WC, Christian ML, Bundy BC. Endotoxin-Free E. Coli-based cell-free protein Synthesis: Pre-expression Endotoxin removal approaches for on-demand Cancer therapeutic production. Biotechnol J. 2019;14:e1800271.
20. Chew CH, Cheng LW, Huang WT, Wu YM, Lee CW, Wu MS, Chen CC. Ultrahigh packing density next generation microtube array membrane: a novel solution for absorption-based extracorporeal endotoxin removal device. J Biomed Mater Res B Appl Biomater. 2020;108:2903–11.
21. Koziel D, Michaelis U, Kruse T. Broad application and optimization of a single wash-step for integrated endotoxin depletion during protein purification. J Chromatogr B Analyt Technol Biomed Life Sci. 2018;1091:101–7.
22. Guan XL, Loh JY, Lizwan M, Chan SCM, Kwan JMC, Lim TP, Koh TH, Hsu LY, Lee BTK. LipidA-IDER to explore the global lipid a repertoire of drug-resistant gram-negative Bacteria. Anal Chem. 2023;95:602–11.
23. Vandenplas ML, Carlson RW, Jeyaretnam BS, McNeill B, Barton MH, Norton N, Murray TF, Moore JN. Rhizobium sin-1 lipopolysaccharide (LPS) prevents enteric LPS-induced cytokine production. J Biol Chem. 2002;277:41811–6.
24. Gorman A, Golovanov AP. Lipopolysaccharide structure and the Phenomenon of Low Endotoxin Recovery. Eur J Pharm Biopharm. 2022;180:289–307.
25. Garcia-Vello P, Di Lorenzo F, Zucchetta D, Zamyatina A, De Castro C, Molinaro A. Lipopolysaccharide lipid A: a promising molecule for new immunity-based therapies and antibiotics. Pharmacol Ther. 2022;230:107970.
26. Xiao X, Sankaranarayanan K, Khosla C. Biosynthesis and structure-activity relationships of the lipid a family of glycolipids. Curr Opin Chem Biol. 2017;40:127–37.
27. Kong Q, Six DA, Liu Q, Gu L, Wang S, Alamuri P, Raetz CR, Curtiss R. 3rd: phosphate groups of lipid A are essential for Salmonella enterica serovar typhimurium virulence and affect innate and adaptive immunity. Infect Immun. 2012;80:3215–24.

28. Tran AX, Stead CM, Trent MS. Remodeling of Helicobacter pylori lipopolysaccharide. J Endotoxin Res. 2005;11:161–6.

29. Cognet I. Expression of recombinant proteins in a lipid A mutant of Escherichia coli BL21 with a strongly reduced capacity to induce dendritic cell activation and maturation. J Immunol Methods. 2003;272:199–210.

30. Mamat U, Wilke K, Bramhill D, Schromm AB, Lindner B, Kohl TA, Corchero JL, Villaverde A, Schaffer L, Head SR, et al. Detoxifying Escherichia coli for endotoxin-free production of recombinant proteins. Microb Cell Fact. 2015;14:57.

31. Liu Q, Li Y, Zhao X, Yang X, Liu Q, Kong Q. Construction of Escherichia coli mutant with decreased endotoxic activity by modifying lipid A structure. Mar Drugs. 2015;13:3388–406.

32. Cardoso VM, Paredes SAH, Campani G, Gonçalves VM, Zangirolami TC. ClearColi as a platform for untagged pneumococcal surface protein A production: cultivation strategy, bioreactor culture, and purification. Appl Microbiol Biotechnol. 2022;106:1011–29.

33. Vereecke N, Kvisgaard LK, Baele G, Boone C, Kunze M, Larsen LE, Theuns S, Nauwynck H. Molecular epidemiology of Porcine Parvovirus Type 1 (PPV1) and the reactivity of vaccine-induced antisera against historical and current PPV1 strains. Virus Evol. 2022;8:veac053.

34. Kiss I, Kovács E, Zádori Z, Mészáros I, Cságola A, Bajnóczi P, Mortensen P, Palya V. Vaccine Protection against Experimental Challenge Infection with a PPV-27a genotype virus in pregnant gilts. Vet Med (Auckl). 2020;11:17–24.

35. Gao Y, Wang H, Wang S, Sun M, Fang Z, Liu X, Cai X, Tu Y. Self-assembly of Porcine Parvovirus Virus-like particles and their application in Serological Assay. Viruses 2022, 14.

36. Wang J, Liu Y, Chen Y, Wang A, Wei Q, Liu D, Zhang G. Large-scale manufacture of VP2 VLP vaccine against porcine parvovirus in Escherichia coli with high-density fermentation. Appl Microbiol Biotechnol. 2020;104:3847–57.

37. Somerville JE Jr., Cassiano L, Darveau RP. Escherichia coli msbB gene as a virulence factor and a therapeutic target. Infect Immun. 1999;67:6583–90.

38. Bishop RE, Gibbons HS, Guina T, Trent MS, Miller SI, Raetz CR. Transfer of palmitate from phospholipids to lipid A in outer membranes of gram-negative bacteria. Embo j. 2000;19:5071–80.

39. Guo L, Lim KB, Poduje CM, Daniel M, Gunn JS, Hackett M, Miller SI. Lipid a acylation and bacterial resistance against vertebrate antimicrobial peptides. Cell. 1998;95:189–98.

40. Brown DB, Muszynski A, Salas O, Speed K, Carlson RW. Elucidation of the 3-O-deacylase gene, pagL, required for the removal of primary β-hydroxy fatty acid from the lipid A in the nitrogen-fixing endosymbiont Rhizobium etli CE3. J Biol Chem. 2013;288:12004–13.

41. Wang X, Karbarz MJ, McGrath SC, Cotter RJ, Raetz CR. MsbA transporter-dependent lipid A 1-dephosphorylation on the periplasmic surface of the inner membrane: topography of francisella novicida LpxE expressed in Escherichia coli. J Biol Chem. 2004;279:49470–8.

42. Micoli F, Rondini S, Gavini M, Pisoni I, Lanzilao L, Colucci AM, Giannelli C, Pippi F, Sollai L, Pinto V, et al. A scalable method for O-antigen purification applied to various Salmonella serovars. Anal Biochem. 2013;434:136–45.

43. Chiu TW, Peng CJ, Chen MC, Hsu MH, Liang YH, Chiu CH, Fang JM, Lee YC. Constructing conjugate vaccine against Salmonella Typhimurium using lipid-A free lipopolysaccharide. J Biomed Sci. 2020;27:89.

44. Hartley JL, Adams GA, Tornabene TG. Chemical and physical properties of lipopolysaccharide of Yersinia pestis. J Bacteriol. 1974;118:848–54.

45. Masuko T, Minami A, Iwasaki N, Majima T, Nishimura S, Lee YC. Carbohydrate analysis by a phenol-sulfuric acid method in microplate format. Anal Biochem. 2005;339:69–72.

46. Islam MA, Pröll M, Hölker M, Tholen E, Tesfaye D, Looft C, Schellander K, Cinar MU. Alveolar macrophage phagocytic activity is enhanced with LPS priming, and combined stimulation of LPS and lipoteichoic acid synergistically induce pro-inflammatory cytokines in pigs. Innate Immun. 2013;19:631–43.

47. Ryu JK, Kim SJ, Rah SH, Kang JI, Jung HE, Lee D, Lee HK, Lee JO, Park BS, Yoon TY, Kim HM. Reconstruction of LPS transfer Cascade reveals structural determinants within LBP, CD14, and TLR4-MD2 for efficient LPS recognition and transfer. Immunity. 2017;46:38–50.

48. Rajaiah R, Perkins DJ, Ireland DD, Vogel SN. CD14 dependence of TLR4 endocytosis and TRIF signaling displays ligand specificity and is dissociable in endotoxin tolerance. Proc Natl Acad Sci U S A. 2015;112:8391–6.

49. Dogan MD, Ataoglu H, Akarsu ES. Effects of different serotypes of Escherichia coli lipopolysaccharides on body temperature in rats. Life Sci. 2000;67:2319–29.

50. Peloso ED, Florez-Duquet M, Buchanan JB, Satinoff E. LPS fever in old rats depends on the ambient temperature. Physiol Behav. 2003;78:651–4.

51. Huang X, Wang X, Zhang J, Xia N, Zhao Q. Escherichia coli-derived virus-like particles in vaccine development. NPJ Vaccines. 2017;2:3.

52. Zhao Q, Li S, Yu H, Xia N, Modis Y. Virus-like particle-based human vaccines: quality assessment based on structural and functional properties. Trends Biotechnol. 2013;31:654–63.

53. Wang K, Zhou L, Chen T, Li Q, Li J, Liu L, Li Y, Sun J, Li T, Wang Y, et al. Engineering for an HPV 9-valent vaccine candidate using genomic constitutive overexpression and low lipopolysaccharide levels in Escherichia coli cells. Microb Cell Fact. 2021;20:227.

54. Deng G, He H, Chen Z, OuYang L, Xiao X, Ge J, Xiang B, Jiang S, Cheng S. Lianqinjiedu decoction attenuates LPS-induced inflammation and acute lung injury in rats via TLR4/NF-κB pathway. Biomed Pharmacother. 2017;96:148–52.

55. Schülke S, Flaczyk A, Vogel L, Gaudenzio N, Angers I, Löschner B, Wolfheimer S, Spreitzer I, Qureshi S, Tsai M, et al. MPLA shows attenuated pro-inflammatory properties and diminished capacity to activate mast cells in comparison with LPS. Allergy. 2015;70:1259–68.

56. Wang Y, Hosomi K, Shimoyama A, Yoshii K, Nagatake T, Fujimoto Y, Kiyono H, Fukase K, Kunisawa J. Lipopolysaccharide Derived from the lymphoid-resident commensal Bacteria alcaligenes faecalis functions as an effective nasal adjuvant to augment IgA antibody and Th17 cell responses. Front Immunol. 2021;12:699349.

57. Ji Y, An J, Hwang D, Ha DH, Lim SM, Lee C, Zhao J, Song HK, Yang EG, Zhou P, Chung HS. Metabolic engineering of Escherichia coli to produce a monophosphoryl lipid a adjuvant. Metab Eng. 2020;57:193–202.

58. Mata-Haro V, Cekic C, Martin M, Chilton PM, Casella CR, Mitchell TC. The vaccine adjuvant monophosphoryl lipid A as a TRIF-biased agonist of TLR4. Science. 2007;316:1628–32.

Publisher's Note